A simple algorithm for yield estimates: Evaluation for semi-arid irrigated winter wheat monitored with green leaf area index

Benoît Duchemin, Philippe Maisongrande, Gilles Boulet, Iskander Benhadj

Available online at www.sciencedirect.com
ScienceDirect
Environmental Modelling & Software 23 (2008) 876–892
Environmental Modelling & Software
www.elsevier.com/locate/envsoft

A simple algorithm for yield estimates: Evaluation for semi-arid irrigated winter wheat monitored with green leaf area index

Benoît Duchemin [a,*], Philippe Maisongrande [b], Gilles Boulet [a], Iskander Benhadj [a]

[a] IRD—U.M.R. CESBIO (CNES/CNRS/IRD/UPS), 18 Avenue Edouard Belin, bpi 2801, 31401 Toulouse Cedex 9, France
[b] CNES—U.M.R. CESBIO (CNES/CNRS/IRD/UPS), 18 Avenue Edouard Belin, bpi 2801, 31401 Toulouse Cedex 9, France

Received 27 July 2006; received in revised form 11 June 2007; accepted 3 October 2007
Available online 3 December 2007

Abstract

In this study we investigated the perspective offered by coupling a simple vegetation growth model and ground-based remotely-sensed data for the monitoring of wheat production. A simple model was developed to simulate the time courses of green leaf area index (GLAI), dry above-ground phytomass (DAM) and grain yield (GY). A comprehensive sensitivity analysis has allowed addressing the problem of model calibration, distinguishing three categories of parameters: (1) those, well known, derived from the present or previous wheat experiments; (2) those, phenological, which have been identified for the wheat variety under study; (3) those, related to farmer practices, which has been adjusted field by field. The approach was tested against field data collected on irrigated winter wheat in the semi-arid Marrakech plain. This data set includes estimates of GLAI with additional DAM and GY measurements. The model provides excellent simulations of both GLAI and DAM time courses. GY space variations are correctly predicted, but with a general underestimation on the validation fields. Despite this limitation, the approach offers the advantage of being quite simple, without requiring any data on agricultural practices (sowing, irrigation and fertilisation). This makes it very attractive for operational application at a regional scale. This perspective is discussed in the conclusion.

Keywords: Crop model; Sensitivity; Irrigated wheat; Production; Yield; Leaf area index

1. Introduction

Irrigated agriculture represents a major contribution to food security, producing nearly 40 percent of food and agricultural commodities on 17% of cultivated lands (FAO, 2002). Irrigated areas, which have almost doubled in recent decades, significantly contribute to the increase of global production. The scope for further irrigation development to meet food requirements in the coming years is, however, severely constrained by decreasing water resources. In particular, serious water shortages occur in semi-arid areas as existing resources reach full exploitation. A challenging objective is thus to ensure food security in a sustainable way of these regions. The design of operational tools that would provide decision-makers with regional estimates of crop production could help to reach this objective. Quantifying crop production at a regional scale would facilitate the monitoring of irrigation efficiency and crop water use. In these regards, the scientific community has paid an increasing interest on approaches based on agro-ecological process models and remote sensing observations (Moulin et al., 1998; Pellenq and Boulet, 2004; Olioso et al., 2005). Models continuously simulate crop development and growth, while satellite imagery provides with space and time regular observations of some biophysical variables of canopies such as the green leaf area index or the fraction of absorbed photosynthetically active radiation (Bastiaanssen et al., 2000; Scotford and Miller, 2005). Approaches based on the combination of modelling and remote sensing thus offers strong opportunities for the monitoring at a regional scale (Clevers et al., 2002; Lobell et al., 2003; Verhoef and Bach, 2003; de Wit et al., 2004; Mo et al., 2005).

* Corresponding author. Tel.: +33 5 61 55 85 01; fax: +33 5 61 55 85 00.
E-mail address: duchemin@ird.fr (B. Duchemin).

1364-8152/$ - see front matter © 2007 Elsevier Ltd. All rights reserved.
doi:10.1016/j.envsoft.2007.10.003

A lot of process-based crop models have been developed in the recent years (see comparisons and reviews in Jørgensen, 1994; Jamieson et al., 1998 or Eitzinger et al., 2004). These models simulate crop development, growth and yield on the basis of the interaction between agro-environmental conditions and plant physiological processes such as photosynthesis, respiration, evapotranspiration and N-uptake. The complexity of these models is increasing because they include either new processes or new details for their description. Although the performance and accuracy of crop models have continuously made progresses over the past few years, applications for yield forecasting over large areas (10 km^2 to 100,000 km^2) have encountered a number of limitations since most of the models were initially conceived for local/field-scale applications (Boote et al., 1996; Faivre et al., 2004; de Wit et al., 2005). Two major limitations are basically pointed out. Firstly, there are generally a large number of model parameters compared to the amount of observation available for their identification. This makes optimisation procedure difficult to operate, since good fits may be achieved for many combinations of the parameters values. Thus, prior (imperfect) information on parameters is required. This results in simulation errors and reduction of the predictive capacity of models (Franks et al., 1997; Wallach et al., 2002). Secondly, it is difficult to cope with the lack of adequate and sufficient input data to run the model at a regional scale. This typically concerns data related to technical practices such as crop calendar as well as irrigation and fertilisation schedules, which know large space and time variations. As an example, Mo et al. (2005) assume uniform irrigation dates and optimal fertilisation over a 90,000 km^2 area; these authors conclude that more timely agronomic information are needed to improve the reliability of yield prediction. An alternative for regional application is to consider simple algorithms which are able to deal with a strong heterogeneity compared to more complex models that treat the surface as homogeneous (Franks et al., 1997). There is thus a large place for testing simple models being specifically designed for the assimilation of remote sensing data.

Amongst the simplest approaches, the theory of light-use-efficiency (Monteith, 1977) has provided a basis to simulate canopy light interception and dry mass production. This theory offers a strong opportunity to be tested in combination with satellite imagery in the optical domain. Indeed, there is an obvious link between surface reflectances and plant light absorption. This link has been widely used to predict dry matter production on natural ecosystems, especially grassland in the Sahelian pastoral zone with the help of coarse spatial resolution satellite data (e.g. Tucker, 1996). For irrigated crop lands, the implementation of such approach is complicated since the growing season varies according to agricultural practices. To track the variability in crop development and production, the use of high spatial resolution satellite data appears more adequate. Lobell et al. (2003) have performed such an analysis on the large irrigated Yaqui Valley (North-West of Mexico) using Landsat-TM images, but the number of images per growing season was limited, and rough estimates of planting dates performed. The design, from now or in a near future, of Earth Observation Systems designed to provide both high spatial resolution (~10 m) and frequent time of revisit (~1 day)—such as RHEA (Dedieu et al., 2003) or FORMOSAT-2 (Chern et al., 2001)—should make improvement possible.

In this context, this study investigates the perspectives offered by the availability of times series of a key biophysical variable (leaf area index) for the monitoring of phytomass production and grain yield of cereal crops. The investigation is based on the "Simple Algorithm For Yield estimate" (SAFY) model, which was specifically developed for this work. The main idea is to use the model to represent well-known processes involved in crop development and growth, with the requirement that these processes can be simulated using standard data, i.e. climatic data and optical imagery (which provides estimates of leaf area index). The model simulates the increase of the dry above-ground phytomass based on the light-use efficiency theory of Monteith (1977), with an account of the dynamics of green leaves and of the effect of temperature. In contrast, the transfers of water and nutriments between the soil and the plant were not explicitly simulated, because of the inability to provide a spatial distribution of the complete set of parameters, initial conditions and input data in case of regional applications. The impact of water and nitrogen stresses is believed to be adjusted from leaf area observations through one main parameter, which is named effective light-use efficiency. It has thus been assumed that the dynamics of green leaves is a good tracer of these agro-environmental stresses.

The objective of this article is threefold: (1) to present the SAFY model; (2) to develop a robust method for its control from time series of green leaf area index; (3) to evaluate this method using data collected over semi-arid wheat crops under a large range of irrigation and fertilisation schedules. The article is organised as follows. The region of interest, the fields of study and the experimental data set are first presented. Then the SAFY model is described, along with a discussion on the parameters that can be identified from literature or field data with satisfying accuracy. The calibration of the remaining parameters is discussed in Section 4, with emphasis on the problem of equifinality and over-parameterisation. Section 5 presents the model evaluation, followed by concluding remarks.

2. The experimental data set

The region of interest is the Haouz plain which surrounds the Marrakech city in the Centre of Morocco. The plain is enclosed between the 'Jbilet' hills at North and the High-Atlas mountain range at South. The High-Atlas, which culminates up to 4000 m above the mean sea level at the Toubkal summit, is the water bank which supplies several big irrigated areas in the plain (Chaponnière et al., 2005).

The experiment took place in an irrigated area of 2800 ha located in the Haouz plain, 40 km East of Marrakech. The area is managed by a regional public agency (ORMVAH: *Office Régional de Mise en Valeur Agricole du Haouz*), which

is in charge of dam water distribution. Field data were collected during two successive agricultural seasons, years 2002–2003 and 2003–2004. This area as well as the first-year experimental set-up has been fully presented in Duchemin et al. (2006). Its main characteristics are the following: cereal crops are dominant, mostly wheat; soils are homogeneous with dominant clay, rather deep (around 1 m) and poor in organic matter (<2%); climate is of semi-arid continental type, with low and irregular rainfall (~240 mm year^{-1}), temperatures moderately low in winter and very high in summer, and a very high evaporative demand (~1500 mm year^{-1}).

2.1. Fields of study

The fields of study are located in Fig. 1 and presented in Table 1. A total of 17 fields have been monitored, 9 during the 2002/2003 and 8 during the 2003/2004 agricultural season. They were labelled C1 to C9 the first season and V1 to V8 the second season as they were used to calibrate and validate the SAFY model, respectively. There are also referred to as calibration and validation fields hereinafter.

All fields were cropped with a short-cycle durum wheat variety suitable for semi-arid conditions and commonly used in the Marrakech plain (ORMVAH technical document). The sowing dates ranged from mid-November to mid-January, with a delay of up to one month between the 2003–2004 season and the 2002–2003 season (Table 1). At the beginning of both season three irrigation rounds were decided on by ORMVAH, but the amount of water supplied was doubled the second season (60 mm per round in 2004 instead of 30 mm in 2003) because the dam level was higher. Fertilisation practices have been highly variable: no fertilisers were applied on the calibration fields except on C5 at flowering time, while 60% of the validation fields were fertilised at sowing (Table 1).

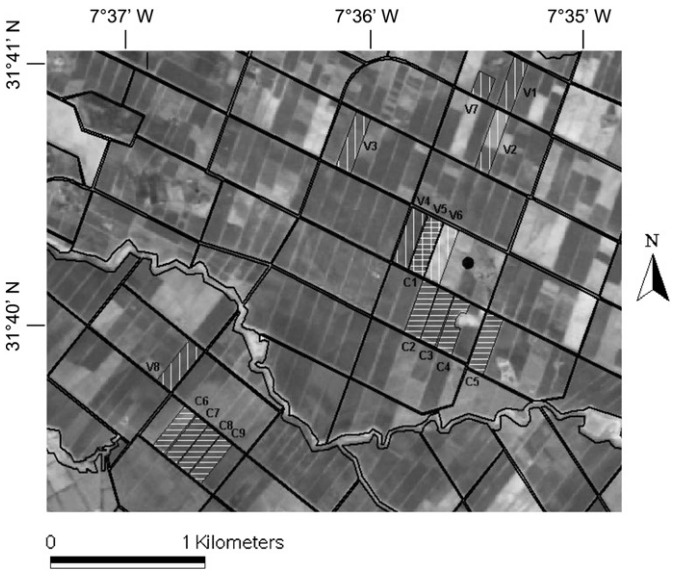

Fig. 1. Location of the fields of study on a Quickbird panchromatic image. Hatched areas with horizontal and vertical lines indicate the calibration (C1 to C9) and validation (V1 to V8) fields, respectively. The black lines delimitate the irrigation units. The black disc highlights the location of the meteorological station.

During the experiment a meteorological station was installed in the vicinity of the fields of study (Fig. 1). The 2002–2003 and 2003–2004 wheat seasons appeared rather comparable in terms of climate (Fig. 2). Because of exceptional rainfall in November (more than 130 mm), both seasons were more humid than usual, with accumulated rainfall close to 380 mm for November to May. The rainfall knows a bimodal distribution with two peaks at the beginning of December and April. The climate was slightly more rainy in 2003–2004 than in 2002–2003 but rainfall events were more irregular the second year, with no rain from mid-December to end of February and late precipitation (40 mm in May). Mean air temperature varied on average from 10 °C in January to more than 20 °C in May. The climate was hotter in 2002–2003 than in 2003–2004, slightly at the beginning of the season, more significantly in May. The evaporative demand logically followed the same trend. According to the reference evapotranspiration ETo (Penman–Monteith equation adapted by FAO for well-watered grass, see Allen, 2000), the two years look roughly comparable until May: ETo was around 2 mm day^{-1} until end of January, then it varied between 2 and 5 mm day^{-1} between February and April. The main difference between the two seasons occurred later with very high ETo values between 6 and 7 mm day^{-1} in May 2003. This explains why the seasonal evaporative demand was 50 mm larger in 2002–2003 than in 2003–2004.

2.2. Green leaf area index (GLAI) and grain yield (GY)

During the 2002/2003 agricultural season, the Green leaf area index (GLAI) was monitored through reflectances data acquired with a hand-held radiometer (Duchemin et al., 2006). We used a MSR87 multispectral radiometer (Cropscan Inc., USA) to measure both incoming and reflected radiation over the spectral bands of LandSat Thematic Mapper (TM) sensor. The red (0.63–0.69 μm) and near-infrared (0.76–0.90 μm) reflectances were used to calculate the Normalised difference vegetation index (NDVI). The comparison with direct metric measurements has allowed establishing an exponential relationship between GLAI and NDVI.

During the 2003/2004 agricultural season, GLAI was derived from hemispherical digital photography based on the analysis of canopy gap fraction (see the review by Jonckheere et al., 2004). For this analysis we strictly followed the procedure designed by Welles and Norman (1991) for the LI-COR LAI-2000 plant canopy analyser instrument. This technique was inter-calibrated with direct measurements and NDVI estimates performed the first season.

At the end of May of both seasons, grain maturity was reached and grain yield (GY) was estimated by ORMVAH technicians. These estimates accounted for yield loss due to the harvesting technique, around 20% of the total yield. The second season cutting and weighting of wheat plants were additionally performed to monitor the dynamics of dry aerial phytomass (V5 field only, on a 10-day basis) and to estimate

Table 1
Fields of study, agricultural practices and grain yield

Field	Agricultural season	Sowing date	Irrigation	Fertilisation (kg ha^{-1})	Grain yield (t ha^{-1})[e]	
					ORMVAH estimates	Field measurements
C1	2002–2003	Dec 18			2.5–3	
C2		#Jan 15[a]	Three events 30 mm each		0.7–1	
C3					0.7–1	
C4					0.7–1	
C5		Jan 11	Six events[b]	100[c]	1.8–2.2	
C6		# Dec 15[a]	Three events 30 mm each		1.5–2	
C7					2.5–3	
C8					2.5–3	
C9					2–2.5	
Average yield value					*1.87*	
V1	2003–2004	Nov 21	Three events 60 mm each		2–2.5	1.6 (0.4)
V2		Nov 21		50[d]	2.5–3	3.4 (1.7)
V3		Dec 15			2–2.5	2.8 (0.8)
V4		Dec 19		100[d]	1.8 – 2.2	2.3 (2.3)
V5		Dec 19		100[d]	3–3.5	4.3 (1.9)[f]
V6		Dec 19		100[d]	3.5–4	3.9 (1.3)
V7		Dec 20			1–1.5	2.2 (1.0)
V8		Dec 24		100[d]	2–2.5	2.5 (1.4)
Average yield value					*2.53*	*2.9 (1.4)*

[a] The exact sowing date is unknown.
[b] The farmer was asked for supplementary irrigation to avoid drought.
[c] Fertilisers were applied at flowering time.
[d] Fertilisers were applied just before sowing.
[e] Left column: range correspond to ORMVAH estimates right column: average values and standard deviation (in parenthese) derived from field measurements.
[f] Measurement of the dry aerial phytomass have also been performed every 10 days on this field.

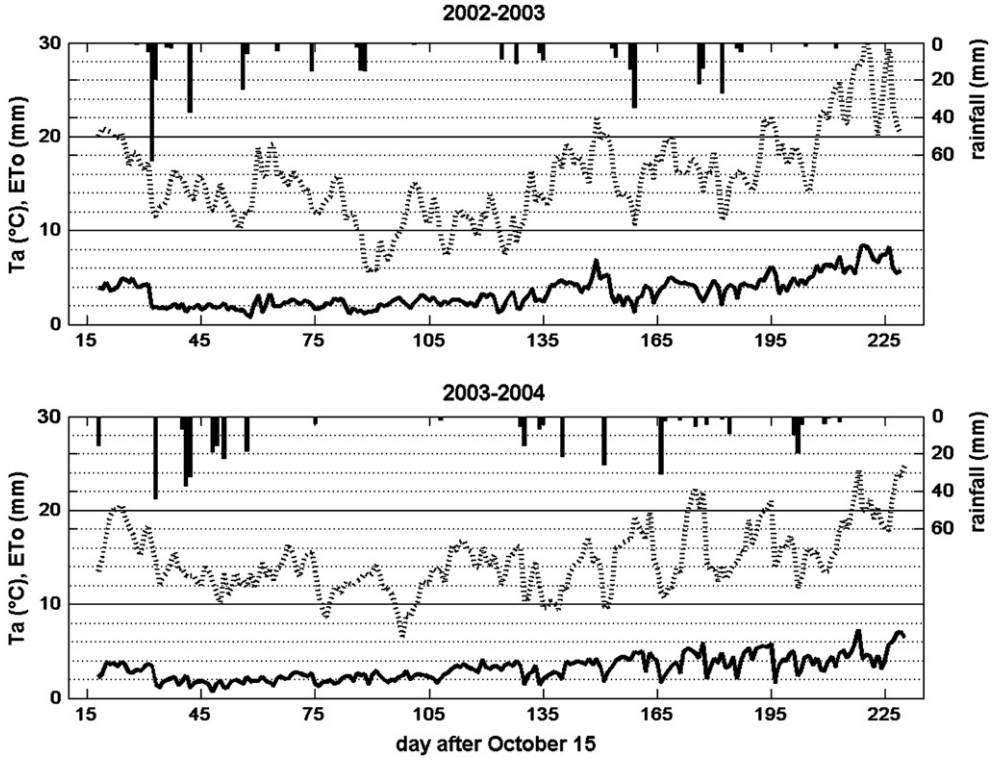

Fig. 2. Time courses of main climatic variables on the area of study during 2002/2003 (top) and 2003/2004 (bottom) agricultural seasons: daily mean air temperature (dotted lines) and reference evapotranspiration (full lines) are associated to the Y-left axis; rainfall (bars) is associated to Y-right axis.

the final grain yield (all fields). GY was measured following the protocol detailed by Hadria et al. (2007), and varied from 0.85 to 4.3 t ha^{-1} (Table 1). Yield values were much lower than those observed in other wheat experiments, even under semi-arid climate (e.g. Lobell et al., 2003; Rodriguez et al., 2004) or drought conditions in temperate climate (e.g. Jamieson et al., 1998; Clevers et al., 2002). The probable main cause is nitrogen stress (Hadria et al., 2007).

The analysis of yield data in Table 1 allows pointing out the difficulty to get accurate estimates of grain yield in the condition prevailing during the experiment. There is a large scatter of measurements due to the high heterogeneity of wheat canopy, and the standard deviation can be as large as the average value (e.g. field V4). Estimates by ORMVAH technicians moderately match field measurements, with a correlation coefficient of 0.81 and large differences around 1 t ha^{-1} in two cases (fields V5 and V7). The bias of 0.4 t ha^{-1} between the two techniques is coherent with the fact that ORMVAH estimates accounts for yield loss during harvest.

3. Model presentation

Monteith (1977) has developed a simple theory to link the production of total dry phytomass and the photosynthetically active portion of solar radiation (PAR) absorbed by plants. The SAFY (Simple Algorithm For Yield estimates) model uses this relationship. It operates at a daily time step from the day of plant emergence (D_0) to the day of complete leaf senescence. During this period, the phytomass production is driven by the incoming PAR radiation absorbed by leaves, with two successive phenological phases: (1) leaf extent; (2) grain filling.

3.1. Formalisms

The SAFY model includes three sub-sets of equations to simulate the time courses of the dry above-ground mass, the Green Leaf Area Index and the Grain Yield. The DAM variable refers to the total aerial phytomass, grains excepted. The climatic forcing includes daily incoming global radiation and daily average air temperature. The notations and units of the main variables and parameters are summarised in Table 2. The equations of the model are detailed below. The model has been developed in MATLAB code and is available upon request to the corresponding author.

3.1.1. Dry above-ground mass (DAM)

The phytomass increases during the period of photosynthetic activity, from an initial value (DAM_0) at plant emergence to a final value when leaf senescence ends. During this period, the production of dry above-ground mass (ΔDAM) is driven by incoming global radiation Rg through the following three factors: (1) the climatic efficiency ε_C, which is the ratio of incoming photosynthetically active to global radiation; (2) the light-interception efficiency ε_I, which is the fraction of photosynthetically active radiation that is absorbed by the canopy (APAR); (3) the effective light-use efficiency ELUE, which is the ratio of photochemical energy produced as DAM from APAR. In addition, ΔDAM is affected by the daily average of air temperature (Ta) through the temperature-stress-function F_T. This leads to:

Table 2
Parameters and variables of the SAFY model (notation and identification)

	Description	Notation	Unit	Value	Source
	Input variables				
	Daily incoming global variation	Rg	MJ m^{-2} d^{-1}		Meteorological station
	Daily mean air temperature	Ta	°C		Meteorological station
	Parameters				
1st	Initial dry above-ground mass	DAM_0	g m^{-2}	4.5	Identified as initial green leaf area index of 0.1
	Climatic efficiency	ε_C	–	0.48	Varlet-Grancher (1982)
	Light-interception coefficient	K	–	0.5	Arora (1998); Brisson (1998); Meinke (1998)
	Minimal temperature for growth	Tmin	°C	0	Porter (1999)
	Optimal temperature for growth	Topt	°C	20	Porter (1999)
	Maximal temperature for growth	Tmax	°C	37	Porter (1999)
	Specific leaf area	S_{La}	m^2 g^{-1}	2.2×10^{-2}	Measured at field
2nd	Partition-to-leaf function: parameter 1	P_{La}	–	15.73×10^{-2}	Calibrated
	Partition-to-leaf function: parameter 2	P_{Lb}	–	1.96×10^{-3}	Calibrated
	Sum of temperature for senescence	S_{TT}	°C	1008	Calibrated
	Rate of senescence	Rs	°C day^{-1}	6875	Calibrated
	Rate of grain filling	Py	°C^{-1}	5.1×10^{-3}	Calibrated
3rd	Day of plant emergence	D_0	day	Local	To be adjusted field-by-field
	Effective light-use efficiency	ELUE	g MJ^{-1}	Local	To be adjusted field-by-field
	Output variables				
	Green leaf area index	GLAI	m^2 m^{-2}		
	Dry above-ground phytomass	DAM	g m^{-2}		
	grain yield	GY	g m^{-2}		

Parameters are presented in 3 groups according to the method used for their identification, discussed in Section 3.2.

$$\begin{aligned}\Delta DAM &= Rg \cdot \varepsilon_C \cdot \varepsilon_I \cdot ELUE \times F_T(Ta) \\ &= APAR \times ELUE \times F_T(Ta)\end{aligned} \quad (1)$$

The light-interception efficiency ε_I depends on the green leaf area index (GLAI) and a light-interception coefficient k through the well-known Beer's law:

$$\varepsilon_I = 1 - e^{-k \times GLAI} \quad (2)$$

Both high and low temperatures decrease the rate of phytomass production (Porter and Gawith, 1999). This effect is accounted for by introducing the air temperature (Ta) in 2nd-degree polynomials determined by an optimal temperature for crop functioning (Topt) and two extreme values (Tmin and Tmax) beyond which the plant growth stops (after Brisson et al., 2003). This leads to:

$$\begin{aligned}F_T(Ta) &= 1 - [(Topt - Ta)/(Topt - Tmin)]^2 && \text{if } Tmin < Ta < Topt \\ &= 1 - [(Ta - Topt)/(Tmax - Topt)]^2 && \text{if } Tmax > Ta > Topt \\ &= 0 && \text{if } Ta < Tmin \text{ or } Ta > Tmax\end{aligned} \quad (3)$$

3.1.2. Green leaf area index (GLAI)

The dynamics of green leaf area index is simulated from the balance between leaf extent during growth ($\Delta GLAI+$, eq. 4) and leaf disappearance during senescence ($\Delta GLAI-$, eq. 6). These two phenological phases are identified based on a degree-day approach from accumulated air temperature (thermal time ΣTa).

During growth, the aerial phytomass production is distributed into leaf and non-leaf mass according to the partition function P_L, then the increase of leaf mass is converted in increase of leaf area ($\Delta GLAI+$) according to the value of the specific leaf area (SLA). This leads:

$$\Delta GLAI+ = \Delta DAM \cdot P_L(\Sigma Ta) \cdot SLA \quad (4)$$

The partition-to-leaf function P_L (eq. 5) is an empirical function of air temperature with 2 parameters (P_{La} and P_{Lb}) adapted from Maas (1993). It is based on the sum of air temperature higher than a base temperature accumulated since plant emergence (ΣTa). The base temperature that affects wheat phenology does not explicitly appear in the equation since it is known to be 0 °C for wheat (Porter and Gawith, 1999; Brisson et al., 2003; Xue et al., 2004). As the P_{La} parameter is close to 0, P_L exponentially decreases with thermal time from a value close to 1 at plant emergence to a value of 0 at the end of the leave production phase.

$$P_L(\Sigma Ta) = 1 - P_{La} \cdot e^{P_{Lb} \cdot \Sigma Ta} \quad (5)$$

The senescence of leaves starts when accumulated air temperature has reached a given threshold S_{TT}. It increases with thermal time at a rate determined by the Rs parameter. It ends when GLAI has returned to a value lower than the initial one, indicating total senescence. This leads to:

$$\begin{aligned}&\text{if } \Sigma Ta > S_{TT} \\ &\quad \Delta GLAI- = GLAI \cdot (\Sigma Ta - S_{TT})/Rs\end{aligned} \quad (6)$$

3.1.3. Grain yield (GY)

The grain filling phase is bounded by the day when foliage production ends and the day when total senescence occurs. During this period, the daily increase of grain yield (ΔGY) is proportional to the total above-ground phytomass, with a constant fraction Py partitioned to grains. This simply leads:

$$\Delta GY = DAM \cdot Py \quad (7)$$

3.2. Parameters

The level of complexity of SAFY is low in the perspective to facilitate the optimisation of unknown parameters using few observations. The parameters are limited in number (14) and can be divided into the three categories highlighted in Table 2 and are discussed below.

In the first category, *a priori* values has been identified according to some previous and the present experimental studies. This was the case for the climatic efficiency (ε_C, eq. 1), the light-interception coefficient (k, eq. 2), the specific values of air temperature related to plant functioning (Tmin, Topt and Tmax, eq. 3), the specific leaf area (SLA, eq. 4) and the initial value of dry above-ground phytomass (DAM_0). Many studies have shown that incoming PAR is roughly half of the incoming global radiation Rg, independently of atmospheric conditions (e.g. Szeicz, 1974). Thus, the climatic efficiency ε_C is nearly constant in space and time, around a value of 0.48 (after Varlet-Grancher et al., 1982). The light-use efficiency is calculated from GLAI based on the light-interception coefficient k. k values range between 0.45 and 0.5 in most of modelling studies. Here we choose the value of 0.5, also used by Arora and Gajri (1998), Meinke et al. (1998) and Brisson et al. (2003). SLA has been measured at field to 0.022 $m^2\,g^{-1}$. This value is consistent with other values found in the literature (0.024 or 0.025 $m^2\,g^{-1}$ in Sinclair and Amir, 1992; Maas, 1993; Arora and Gajri, 1998). Wheat is generally considered to take advantage of an optimum temperature range of 17–23 °C over the entire growing season, with extreme temperatures of 0 °C and 37 °C beyond which growth stops (Porter and Gawith, 1999). Thus the minimal, optimal and

maximal temperatures for wheat growth have been set up to 0, 20 and 37 °C, respectively. Finally, a low initial value of 4.5 g m^{-2} has been identified for the dry above-ground mass at plant emergence. Given the SLA value, the DAM_0 value correspond to an initial GLAI of 0.1 (see eq. 4). The fact of identifying (somehow) arbitrarily this parameter is not critical since it is closely related to the definition of the plant emergence stage (GLAI = 0.1 in this study). Indeed, the model would give comparable results in case of a low initial GLAI value with early plant emergence as in case of a higher initial GLAI value with delayed emergence. Keeping constant the initial DAM value thus allowed gaining consistence in the definition and in the inversion of the date of plant emergence.

The second category includes phenological parameters, which depend on the genetic characteristics of the crop (type and variety). It includes the five parameters that drive the mass partitioning between organs and the change in phytomass status: leaf appearance during growth (P_{La} and P_{Lb}, in eq. 5); beginning and rate of senescence (S_{TT} and Rs, in eq. 6); rate of grain filling (Py, in eq. 7). The four first parameters affect the seasonal pattern—but not the amplitude—of the GLAI time course.

The third category is made of the two last parameters that strongly depend on agro-environmental conditions. The first one is the day of plant emergence (D_0), which occurs generally 1 to 3 weeks after sowing depending on the soil temperature and moisture. The second one is the effective light-use efficiency (ELUE), which is supposed in this study to account for all agro-environmental stresses, temperature excluded. This parameter is expected to give in a simple manner a global level of all these agro-environmental stresses integrated together, which could be an indicator of the performance of agricultural practices, such as the irrigation and fertilisation schedules.

The total number of parameters is 14, amongst which 7 have been obtained from the above mentioned literature, field data or assumptions (1st category in Table 2). We can distinguish the 7 other parameters in terms of their variations in space. Since the life cycle of wheat plants are determined by genetic characteristics, the phenological parameters (2nd category in Table 2) are assumed to be dependent of the wheat variety. Consequently, there are supposed to be constant through the fields of study. However, because their direct measurements are difficult or impossible, they need to be calibrated. The last two parameters (3rd category in Table 2) are highly variable in space as they are directly affected by farmer practices. They required to be adjusted locally, at least at a field scale.

4. Model calibration

In this study, calibration is considered as the procedure of identifying a single optimum parameter set resulting in a simulation that best reproduces several observed variables. Though important, evaluation of crop model parameters has not been fully investigated. More studies have been undertaken on soil-vegetation-atmosphere transfer and hydrological models (Beven and Binley, 1992; Bastidas et al., 1999; Beven, 2001; Wagener et al., 2001; Demarty et al., 2004; Vrugt et al., 2002, 2005). These studies have shown that the calibration of (even simple) models is a complex issue since the parameters are often inter-dependant. Dependency or compensation between parameters causes equifinality or functional similarity (Franks et al., 1997; Beven and Franks, 1999). In particular, this may occur when different sets of parameter values can result in similar simulations of a particular variable while other variables may strongly and inconsistently differ from one simulation to the next, though initial and boundary conditions are kept constant. That is why it is essential to identify the parameters which have a biophysical interpretation based on experimental results, as done for half of the SAFY model parameters (1st category of parameters in Table 2 with the values discussed in the last section). The procedure to identify the remaining parameters is discussed in this section.

4.1. A typical example of parameter compensations

A first attempt to derive the phenological parameters was performed based on the experimental data collected on the C1 field taken as an example. The objective was to retrieve all the non-*a priori*-known parameters that drive the time course of GLAI, i.e. all the parameters of the above-discussed 2nd and 3rd categories except the rate of grain filling which only influences yield. There are 6 such parameters (Table 3): the day of plant emergence (D_0), the two parameters of the partition-to-leave function (P_{La} and P_{Lb}), the two parameters of the senescence function (S_{TT} and Rs), and the effective light-use efficiency (ELUE). All these parameters were calibrated against the GLAI observations collected on the C1 field using the SCEM-UA algorithm (Vrugt et al., 2002). This algorithm is adapted from the SCE-UA global optimisation method (Duan et al., 1992), which has been used extensively and proved to be robust and efficient for the calibration of conceptual rainfall runoff models. The setting of the method was the following: we assumed a uniform prior distribution of the possible parameters (option 3), the number of complexes was 10, the population size was 200, the number of function evaluation was 5000, and the residual error was assumed normally distributed (Gamma = 1). The conditions of application were strictly similar from one optimisation to the next: same formalisms and equations, same *a priori*-known parameters,

Table 3
Parameters targeted for robustness and sensitivity analysis

Description	Notation	Unit	Range of variation
Day of plant emergence	D_0	day	50–150
Leaf partitioning function: parameter 1	P_{La}	–	0.01–0.3
Leaf partitioning function: parameter 2	P_{Lb}	–	5×10^{-4}–1×10^{-2}
Sum of temperature to start senescence	S_{TT}	°C	200–2000
Rate of senescence	R_S	°C day^{-1}	1000–15000
Effective light-use efficiency	ELUE	g MJ^{-1}	0–10

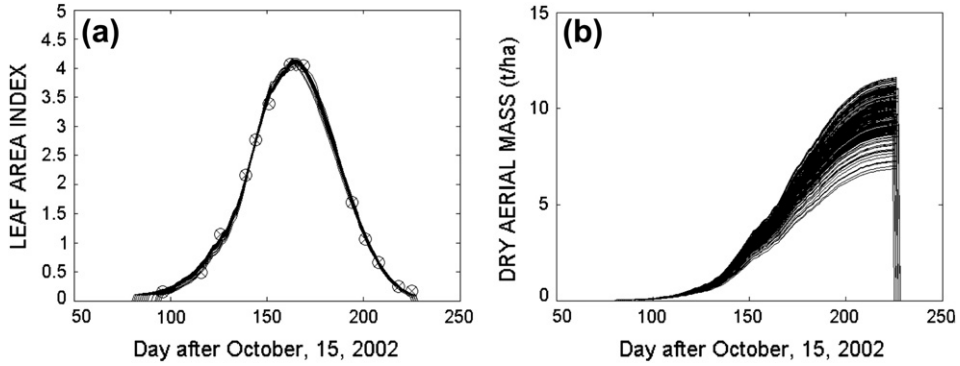

Fig. 3. Time courses of green leaf area index (a) and dry aerial phytomass (b). The simulations have been carried out using 200 sets of the 6 parameters that drive the GLAI time course, each set being calibrated against the GLAI values observed on one field of study (symbols in a).

same climatic forcing, same set of targeted observations. With this setting, the SCEM-UA algorithm was successively applied 200 times with a large range of feasible parameters (see Table 3). For each run, we retained the best parameters set as the one with the best posterior density (i.e. the lowest absolute error between observed and measured values). The result consists in 200 sets of the targeted six parameters associated with simulations of GLAI and DAM time courses, which were analysed using the following statistical indicators:

$$\mathrm{EFF} = 1 - \frac{\sum_{i=1}^{n}(y_{i\mathrm{mod}} - y_{i\mathrm{obs}})^2}{\sum_{i=1}^{n}(y_{i\mathrm{obs}} - \overline{y}_{\mathrm{obs}})^2} \tag{8}$$

(efficiency)

$$\mathrm{RMSE} = \sqrt{\frac{1}{n}\sum_{i=1}^{n}(y_{i\mathrm{mod}} - y_{i\mathrm{obs}})^2} \tag{9}$$

(root mean square error)

$$R = \frac{\sum_{i=1}^{n}(y_{i\mathrm{mod}} - \overline{y}_{\mathrm{mod}})(y_{i\mathrm{obs}} - \overline{y}_{\mathrm{obs}})}{\left\{\left[\sum_{i=1}^{n}(y_{i\mathrm{mod}} - \overline{y}_{\mathrm{mod}})^2\right]\left[\sum_{i=1}^{n}(y_{i\mathrm{obs}} - \overline{y}_{\mathrm{obs}})^2\right]\right\}^{1/2}} \tag{10}$$

(correlation coefficient)

where $y_{i\ \mathrm{mod}}$ is one simulated value, $y_{i\ \mathrm{obs}}$ is one measurement, y_{mod} is the average of simulated values, y_{obs} is the average of measurements.

The result is displayed in Figs. 3 and 4. It appears clearly that the GLAI observations are always accurately captured

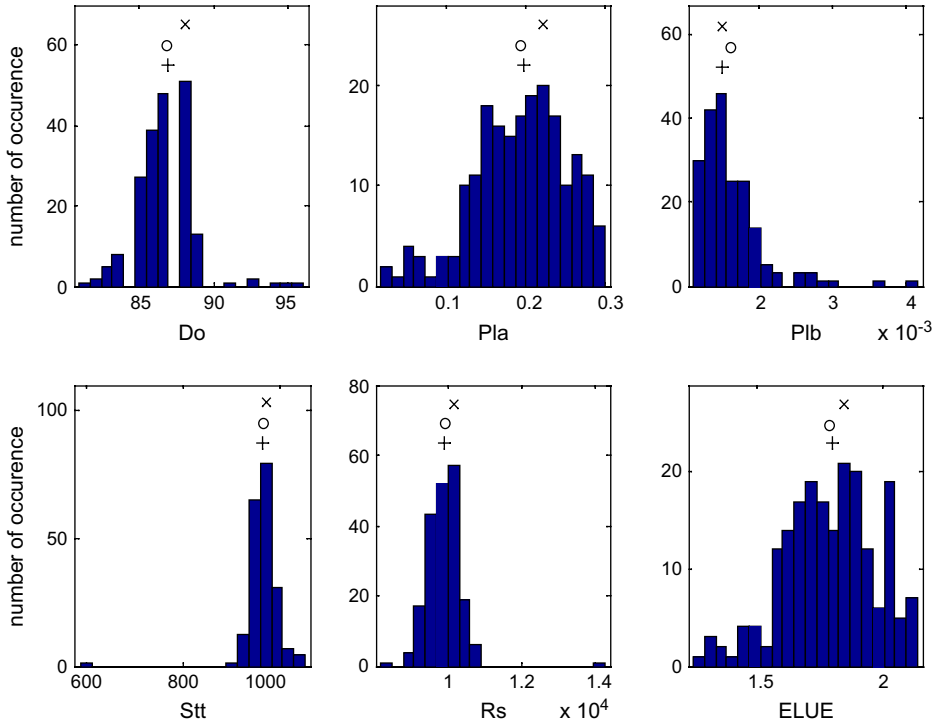

Fig. 4. Histograms of the parameters associated to the 200 simulations displayed in Fig. 3. Symbols indicate the median value (+), the mean value (○) and the value with maximum of occurrence (×).

by the model (Fig. 3a): for the 200 simulations, the root mean square error between observed and simulated GLAI values is on average 0.06 with a maximum of 0.11 (3% of the maximum observed GLAI), and individual errors are lower than this average value for 70% of the 200 cases; the efficiency is always very close to 1 with a minimum value of 0.997. Nevertheless, the parameters may strongly vary from one optimisation to the next. The histograms of the 200 sets of parameters which are compatible with the observed data are displayed in Fig. 4. The relative variations of the parameters, i.e. the ratio of the difference between the maximum and the minimum value to the average value, ranges between 17% for the emergence date (D_0) to almost 200% for the second parameter of the partition-to-leave function (P_{Lb}). These variations result in large discrepancy in the simulations of the dry above-ground phytomass from one set of parameter to the other (Fig. 3b): the final DAM values range from 6.8 to 11.6 t ha^{-1} for the 200 simulations, varying more or less by 50% around the average value (9.7 t ha^{-1}). Indeed, similar simulations of GLAI can be for instance obtained with a high growing rate (high ELUE) in combination with a low biomass allocation to leaf (low P_L), or with less growth (low ELUE) in combination with a high biomass allocation to leaf (high P_L). These non-coherent variations will affect the estimates of grain yield with the same order of magnitude.

This first analysis typically allowed to highlight what is referred to as equifinality in this study: good fits of GLAI may be achieved in many areas of the parameters space, but there is still a consequent uncertainty in the simulations of other variables (DAM and GY). Similar behaviours have been particularly studied by S.W. Franks and K.J. Beven in the case of hydrological and soil-vegetation-atmosphere transfer models (Beven and Binley, 1992; Franks et al., 1997; Beven and Franks, 1999; Beven, 2001).

4.2. Sensitivity analysis

The implication of the equifinality problem is that additional parameters should be identified to calibrate the SAFY model. In order to quantify the respective importance of the parameters as well as their inter-connection, we have carried out one (1D) and two (2D) dimensional sensitivity analysis. The analysis was done from the comparison of simulated and observed GLAI on field C1, with a focus on one or two of the six non *a priori* known parameters that impact on the GLAI time course (see the previous section). The method consisted in choosing one parameter (1D) or a couple of parameters (2D), for which changes in GLAI simulations in response to their variations were systematically analysed.

The 1D analysis was carried out by letting one parameter vary, the five others being kept constant at their median values displayed in Fig. 4. The interval of variation of the targeted parameter was chosen from −50% to +50% of its median value. The result is displayed in terms of errors between simulated and observed GLAI on field C1 (Fig. 5). Taking as an indicator of the sensitivity the maximum value of the root mean square error through the interval of variation (black discs in Fig. 5), the most sensitive parameter appears to be the effective

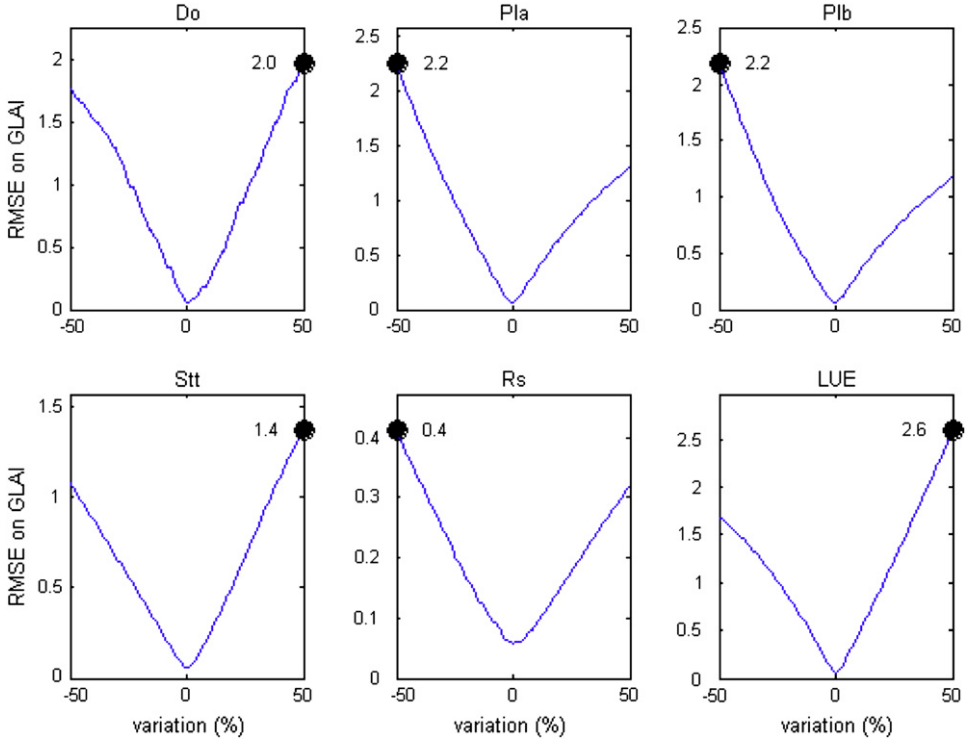

Fig. 5. Results of the 1-D sensitivity analysis. The targeted parameter appears as the title of each subplot. The root mean square error (RMSE) between observed and simulated values of green leaf area index (GLAI) is plotted for each of the six parameters that drive the GLAI time course. Each parameter varies by ±50% around its median values displayed in Fig. 4. Black discs and associated labels highlight maximum errors.

light-use efficiency (ELUE), followed by the two parameters of the partition-to-leave function (P_{La} and P_{Lb}) and the day of plant emergence (D_0), then the parameter that determines the beginning of senescence (S_{TT}), and finally the rate of senescence (Rs).

The 2D analysis was carried out by letting two parameters vary, the four other being constant to their median values displayed in Fig. 4. The intervals of variation of the targeted parameters accounted for the result of the 1D analysis in order to have homogeneous representations of all the 2D-error plots. The result of the 2D analysis is displayed in Fig. 6. When one dimension includes the date of plant emergence (Fig. 6a–e), the RMSE regularly increases in all directions of the 2D-parameter spaces around a minimum value. In other words, the emergence date is the only parameter that appears nearly fully independent. In contrast, the presence of valleys in several plots indicates that one parameter strongly compensates the other, i.e. the two parameters are partly dependent. The strongest compensation occurs between the two parameters of the partition-to-leaves function (Fig. 6f), followed by each of these two parameters and the effective light-use efficiency (Fig. 6i and l), then the two parameters of the senescence function (Fig. 6m), and finally the parameter that determines the beginning of senescence and each of the two parameters of the partition-to-leaves function (Fig. 6g and j).

4.3. Identification of parameters: simulation of leaf area index and grain yield

According to the presentation of the SAFY model and its sensitivity analysis (see Sections 3 and 4.2), it seems justified to calibrate the phenological parameters in priority. Indeed, these parameters depend on the plant genetic characteristics and are thus believed not to vary for a given crop type and variety. Consequently, a single set of parameters should be suitable for all the fields of study which are cropped with the same wheat variety. Furthermore, their determination will limit

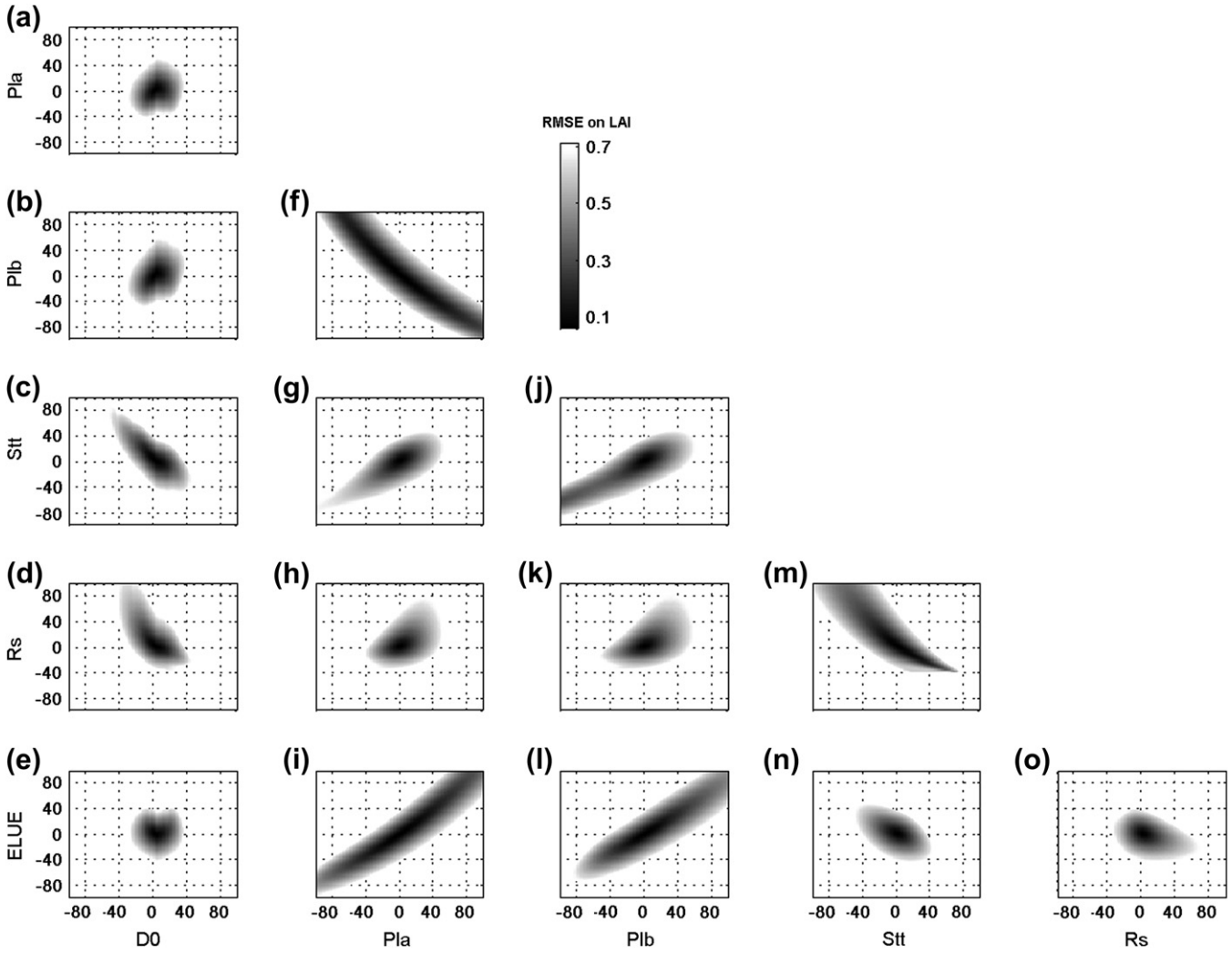

Fig. 6. Results of the 2D-sensitivity analysis. The root mean square errors between observed and simulated green leaf area index are plotted as surfaces for the different couples of parameters used in the simulations (X- and Y-axis). The parameters deviate from their median values (see Fig. 4) by 100% divided by the maximum errors displayed in Fig. 5. The colour bar displays the error ranging from 0.1 to 0.7 with a linear grey scale. Negative Rs values, which are out of the physical definition domain, appear non-gridded in graphs d, h, k, m and o.

ambiguity in the retrieval of the remaining 2 parameters (D_0 and ELUE), which have been found independent (Fig. 6e).

The calibration was based on the experimental data set acquired during the 2002/2003 agricultural season (fields C1 to C9 in Fig. 1 and Table 1). It consisted in the following three-step procedure:

(1) A statistical analysis on 1800 sets of parameters (200 runs for each of the 9 calibration fields) was performed to identify the optimal set of the four—genetic, thus a priori unique—parameters that drives the dynamics of plant leaves (development and senescence);
(2) The same optimisation scheme was used to identify the two remaining parameters (ELUE and emergence date) that control the vegetation growth; however, as these parameters varied with agricultural practices, they have been retrieved field by field; their variations are discussed at the end of this section;
(3) Finally, we adjusted the—unique—parameter that determines the increase of grain weight; in this last step, estimates of grain yield were used as the optimisation objective, whereas in the two previous steps the optimisation objective is only GLAI.

4.3.1. Green leaf area index

There are four parameters that affect the shape of the GLAI time course: the two parameters of the partition-to-leaf function (P_{La} and P_{Lb} in eq. 5) and the two parameters of the senescence function (S_{TT} and Rs, in eq. 6). The procedure for their retrieval was similar to that applied on field C1 (based on the SCEM-UA algorithm, see Section 4.1, Figs. 3 and 4) but generalised to all the calibration fields. The four parameters, together with the day of emergence and the effective light-use efficiency, have been adjusted 200 times for each of the 9 calibration fields. All the retrieved parameters were mixed together, and then one can choose amongst three statistical variables to derive a single value from the resulting histograms: median, mean and maximum of occurrence. Though there are few differences amongst the variables, the use of median values led to the best agreement between observations and simulations. Indeed, the mean value can be affected by unrealistic extreme values, while the maximum of occurrence is not satisfying in case of non-monomodal histogram. This is illustrated in the case of field C1 in Fig. 4: for the P_{Lb} parameter, there is a shift of the mean compared to the median due to several large values; for the P_{La} parameter, the value associated to the maximum of occurrence is significantly different from both the median and the mean value.

The set of P_{La}, P_{Lb}, S_{TT} and Rs median values resulting from the previous analysis is displayed in Table 2. After calibration, simulations were adjusted again on GLAI observations for each individual field, with all the parameters remaining constant and fixed at the values displayed in Table 2 excepted the day of emergence and the effective light-use efficiency. These two parameters have been re-optimised field by field using the SCEM-UA algorithm, which was repeated 50 times for each field, always resulting in the same $D_0 \times$ ELUE couple of values. This finding was expected since the two parameters have been found independent (see Fig. 6e).

The resulting simulations of green leaf area index are plotted together with observations in Fig. 7. The time courses of GLAI are quite well simulated: for the 9 calibration fields efficiencies are on average 0.95 with a minimal value of 0.88 for field C9; the root mean square error between observed and simulated GLAI ranges between 0.08 for field C2 and 0.59 for field C9, representing 3% and 12% of the maximum values, respectively. The maximum errors, which occur on fields C7 and C9, appear firstly linked to underestimation at the end of simulations (see days after 180 in Fig. 7). This underestimation is explained by uncertainty in the retrieval of the day of plant emergence due to a lack of measurements at the beginning of the season (see Section 4.3.3). Large errors are secondly due to the fact that the normalised difference vegetation index saturates for well-developed canopy (see Duchemin et al., 2006), resulting in scatter of high GLAI observations (e.g. day 150, fields C6 to C9).

4.3.2. Grain yield

The six parameters that controls LAI and DAM being now identified, the only unknown parameter is the one that determines the partition of the dry above-ground phytomass into grains (Py, eq. 7). This parameter was adjusted from simulations obtained with a realistic interval of variation with the objective to accurately predict the crop yield. In this objective, we search to minimise the root mean square error between observed and simulated yield values, with this error calculated from the 9 calibration fields. A minimal root mean square error of $0.47\ t\ ha^{-1}$ was found for a Py value equal to $5.1 \times 10^{-3}\ °C^{-1}$. This error represents 25% of the C1 to C9 average yield value ($1.87\ t\ ha^{-1}$, see Table 1).

Observations and simulations of grain yield are plotted together with the GLAI time courses in Fig. 7. The model appears able to track a significant part of yield variation: the correlation coefficient between simulated and observed GY is 0.8 ($R^2 = 0.64$) for the nine calibration fields. GY simulations end within the range of error assumed for ORMVAH estimates, excepted on fields C1 and C7 for which GY appears underestimated by 0.8 and $0.7\ t\ ha^{-1}$, respectively. Although the formalism of the SAFY model to simulate grain yield is quite simple, the accuracy of these results are comparable to that obtained with more complex models (e.g. O'Leary and Connor, 1996; Asseng et al., 1998; Jamieson et al., 1998; Clevers et al., 2002; Brisson et al., 2003).

4.3.3. Day of emergence and light-use efficiency

Table 4 provides with the final values of days of plant emergence (D_0), together with the value of sowing dates collected from the farmers. Sowing and emergence dates are highly correlated ($R^2 = 0.93$), with emergence occurring on average 21 days after sowing. However, there are large variations in the delay between sowing and emergence, which may partly be due to uncertainty in the observations (see Table 1). Excluding the case of field C1, the delay appears to increase

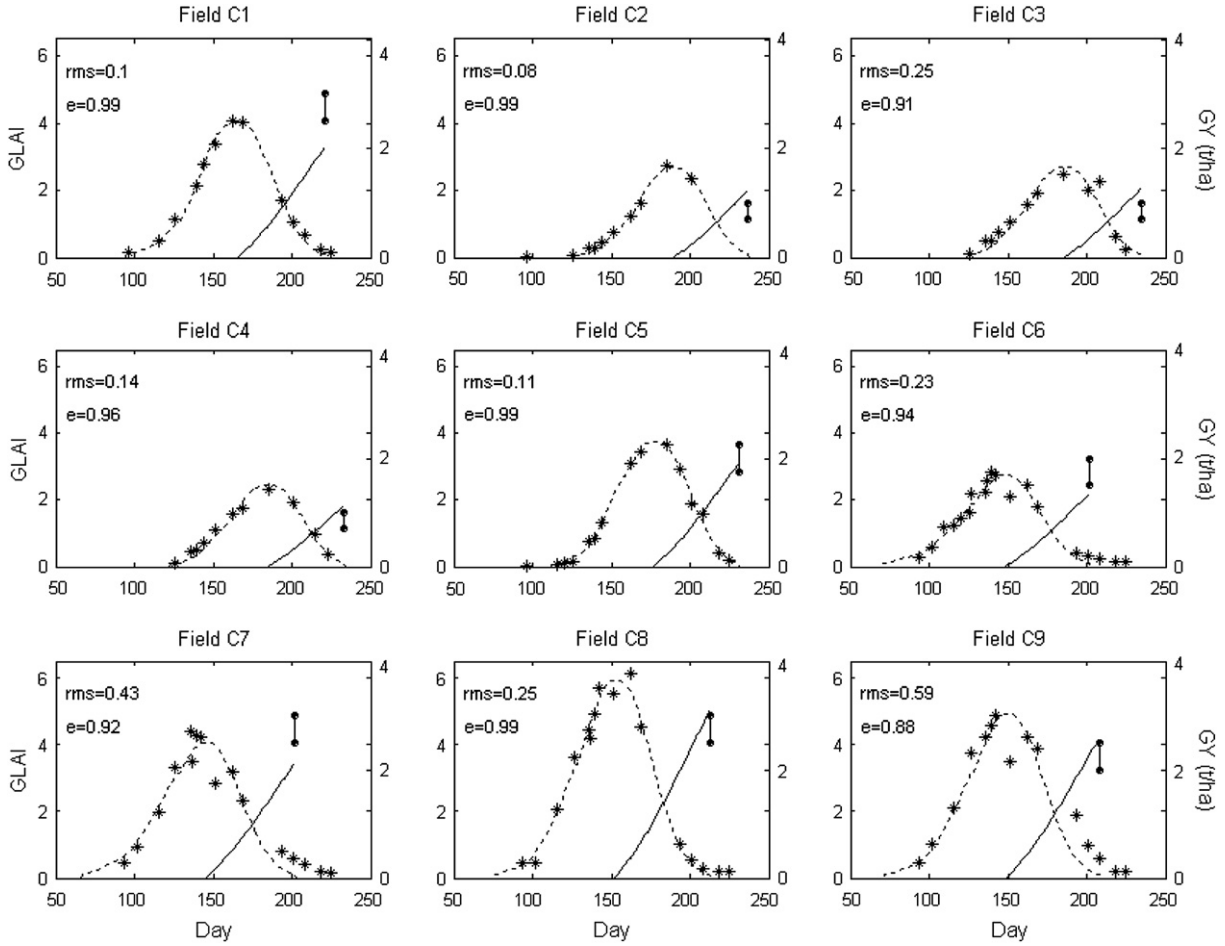

Fig. 7. Observations of green leaf area index (stars) and grain yield (ranges of ORMVAH estimates displayed by vertical lines) together with their respective simulations (lines) after calibration. Each subplot corresponds to one calibration field named in the title. Root mean square error and efficiency between observed and simulated GLAI values are displayed with label 'rms' and 'e', respectively. The days are numbered from October 15, 2002.

by about 10 days for the fields sown in December (C6 to C9) to around 30 days for the fields sown in January (fields C2 to C5). Although these variations are coherent with the fact that both air temperature and soil moisture are higher in December than in January (see Fig. 2, left), the short delays on fields C6 to C9 appears unrealistic. The fitting procedure probably underestimates D_0 on these four fields which have not been monitored at the beginning of the season. This also explains the shift in the simulation of GLAI at the end of leaf senescence (Fig. 7).

The effective light-use efficiency varies between 1.49 and 2.43 g MJ^{-1} (Table 4), in the range found in the literature for the production of wheat above-ground dry mass, e.g. 1.34 to 2.5 g MJ^{-1} (Maas, 1993; Jamieson et al., 1998;

Table 4
Values of the local parameters of the SAFY model (adjusted field by field)

	Calibration fields								
	C1	C2	C3	C4	C5	C6	C7	C8	C9
Day of emergence[a]	Jan 1	Feb 22	Feb 16	Feb 14	Feb 4	Dec 15	Dec 12	Dec 21	Dec 17
	30	*∼38*	*∼32*	*∼30*	*24*	*∼8*	*∼5*	*∼14*	*∼10*
Light-use efficiency	1.89	1.66	1.64	1.49	1.82	1.74	2.13	2.43	2.26
	Validation fields								
	V1	V2	V3	V4	V5	V6	V7	V8	
Day of emergence[a]	Dec 16	Dec 11	Jan 24	Jan 20	Jan 14	Jan 13	Jan 23	Feb 3	
	25	*20*	*36*	*31*	*25*	*24*	*33*	*41*	
Light-use efficiency	2.18	2.37	1.75	1.56	1.94	2.18	1.46	2.19	

[a] Numbers in italics indicate the delay between the sowing day and day of plant emergence (the ∼ symbol is used if the sowing date is not exactly known, see Table 1).

Meinke et al., 1998; O'Connell et al., 2004). Its variation appears consistent with agricultural practices. Firstly, ELUE is higher when sowing is earlier (fields C1 and C6 to C9 compared to others). The advantage of early sowing has been also underlined using the STICS crop model by Hadria et al. (2007). In case of early sowing the plant takes advantage of the first effective rainfalls (3 events with daily rainfall higher than 20 mm between November 15 and December 9, 2002, see Fig. 2, left) and do not suffer from water stress at the end of the season when the evaporative demand reach its maximum values. Amongst the remaining fields (C2 to C5), ELUE is the highest for the field which has been irrigated six times and fertilised (fields C5 compared to C2, C3 and C4, which are all sown Mid-January).

5. Model evaluation

The SAFY model was evaluated against the experimental data set collected on the validation fields during the 2003/2004 agricultural season (V1 to V8 in Fig. 1 and Table 1). The day of emergence and the effective light-use efficiency have been adjusted for each of these fields, with all other parameters remaining constant to their calibrated values (see Table 2). The values of these two parameters are first discussed, then the simulations of the three main output variables (green leaf area index, dry above-ground mass, and grain yield) are analysed.

5.1. Day of emergence and light-use efficiency

The values of days of emergence and effective light-use efficiencies are presented in Table 4. The trends in their variation are common with the calibration fields. Firstly, days of plant emergence and sowing date are highly correlated ($R^2 = 0.92$ in Fig. 8). Secondly, the delay between sowing and emergence increases with the time of sowing: it is on average 22.5 days for the fields sown in November (V1 and V2) against 31.5 days for the fields sown in December (V3 to V8). This delay appears more regular on validation fields than on calibration fields. The effective light-use efficiency ranges between 1.56 and 2.37 MJ^{-1} on the validation fields and shows the same trends than on calibration fields. Its variation between fields appears to be first linked to agricultural practices: the field displaying the highest efficiency (V2) was sown early and fertilised at sowing; the field that displays the lowest efficiency is V7, with late sowing and no fertilisation (see Table 1). However, if these two extreme values correspond to the best and the worst practices, the hierarchy is not so clear for intermediate values. In particular, the differences in practices do not explain the variation in ELUE between the fields V4, V5 and V6, which are juxtaposed and cropped by the same farmer. It is possible here that inaccuracy occurs during the collection of technical itinerary. As additional indicators of the crop behaviour, it would be also interesting to consider other practices such as ploughing or weed/pest controls as well as the field history, but these data were unavailable for most of the fields of study.

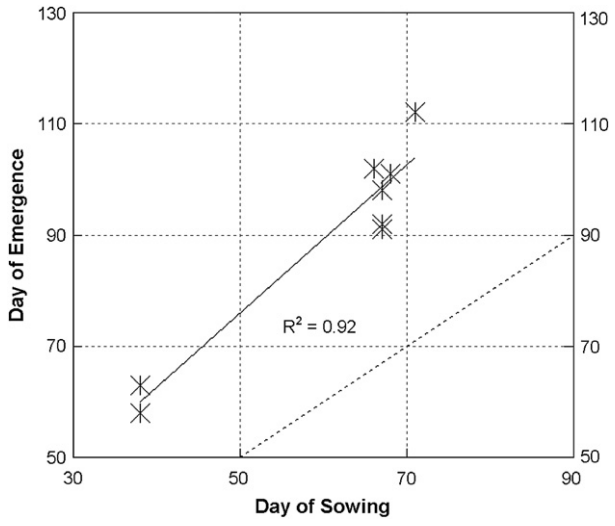

Fig. 8. Comparison between sowing and emergence dates for the validation fields (in number of days after October 15, 2003). The dotted line highlights the X = Y line.

5.2. Green leaf area index

The performance of the SAFY model to simulate GLAI time courses on the validation fields appears quite satisfactory (Fig. 9). The seasonal variation appears as well reproduced as for the calibration fields (compare Figs. 7 and 9), even if the root mean square errors is slightly larger than on the calibration fields (on average 0.4 for the validation fields against 0.24 for the calibration fields). The explanation appears to be first linked to observations: it seems that high GLAI values are more scattered the second season (using hemispherical photography) than the first season (estimates from NDVI). Furthermore, it is clear from Figs. 7 and 9 that GLAI observations are much noisy for well-developed canopies than for scarce vegetation. However, the consequence is limited for the simulation of the crop production since the intercepted radiation saturates for high GLAI values (exponential law in eq. 2).

Despite this, the GLAI seasonal patterns are all well reproduced by the model. This confirms the quality of the calibration of the phenological parameters. In the conditions prevailing in this study, the assumption that these parameters do not depend on water and nitrogen stresses appears valid. This assumption is used in several crop models (e.g. STICS, Brisson et al., 2003), while other models simulate an acceleration of leaf senescence in case of water stress. In the last case, the impact of water stress is nevertheless much larger on the amplitude than on the shape of the GLAI seasonal course (e.g. Jamieson et al., 1998).

The accuracy of GLAI simulations appears comparable to that of other simplified models with a higher degree of liberty during calibration (e.g. 5 parameters adjusted in Maas, 1993). The performance of the SAFY model to simulate GLAI time courses is often much better than that of more complex models (e.g. Pala et al., 1996; Asseng et al., 1998; Jamieson et al.,

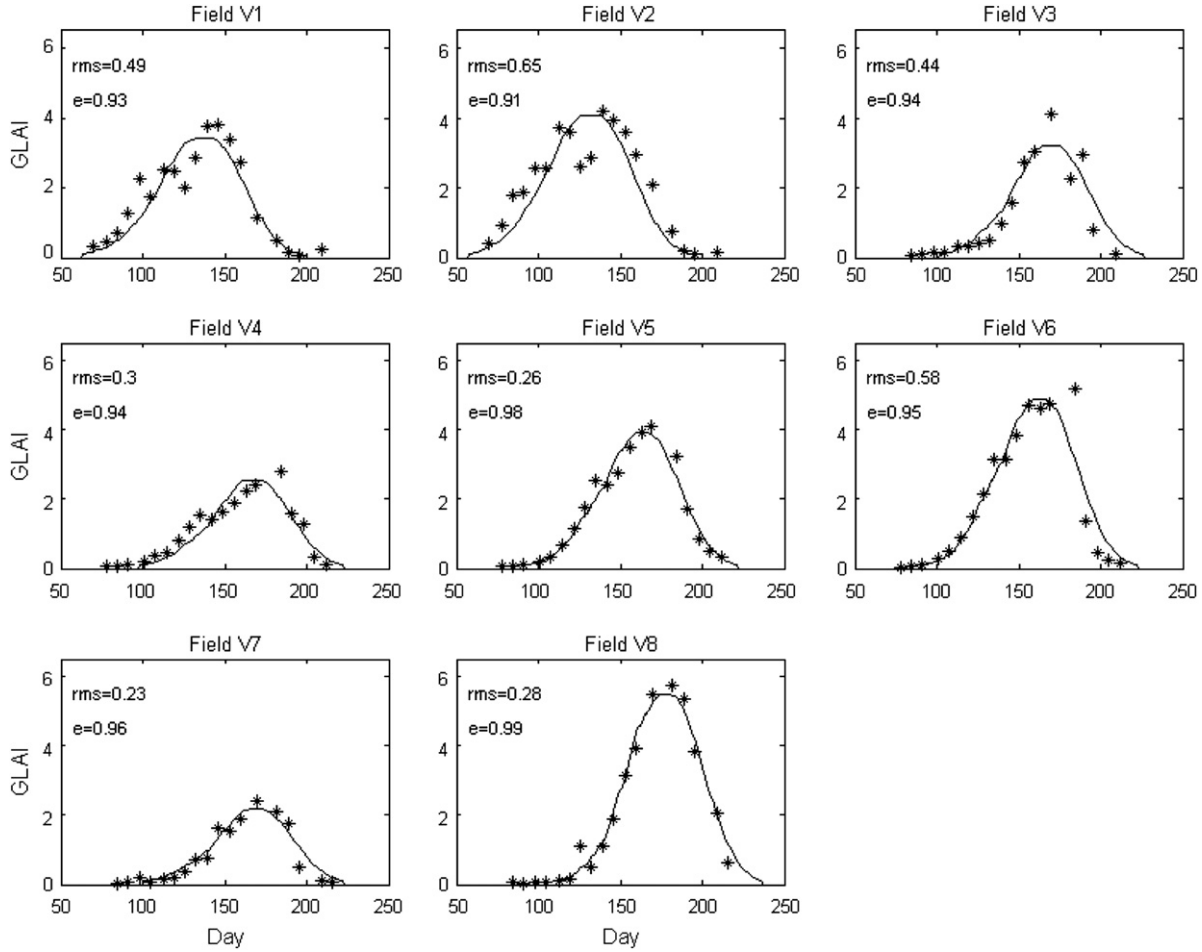

Fig. 9. Times course of observed (stars) and simulated (lines) green leaf area index (GLAI). Each subplot corresponds to one validation field named in the title. Root mean square errors and efficiencies between observations and simulations are displayed with label 'rms' and 'e', respectively. The days are numbered from October 15, 2003.

1998; Meinke et al., 1998; Clevers et al., 2002; Olesen et al., 2002; Panda et al., 2003; Asseng et al., 2004; Rodriguez et al., 2004; Hadria et al., 2007). However, it should be kept in mind that the SAFY model is driven by GLAI observations, which is not always the case in the above-mentioned studies.

These results are quite acceptable regarding the accuracy of leaf area index estimates performed with indirect methods such as remote sensing or hemispherical photography. Indeed, average difference of 30% on wheat GLAI estimates between direct (metric) and indirect methods have been reported during this experiment (Duchemin et al., 2006; see also Weiss et al., 2004 for a review).

5.3. Grain yield

The SAFY model moderately reproduces the variation observed from one validation field to the next (Fig. 10). The correlation coefficient between simulation and visual estimates is around 0.69 ($R^2 = 0.48$), slightly lower than for the calibration fields. Furthermore, the model clearly underestimates grain yield, by on average 0.5 t ha^{-1} when compared to ORMVAH estimates and 0.9 t ha^{-1} when compared to field measurements.

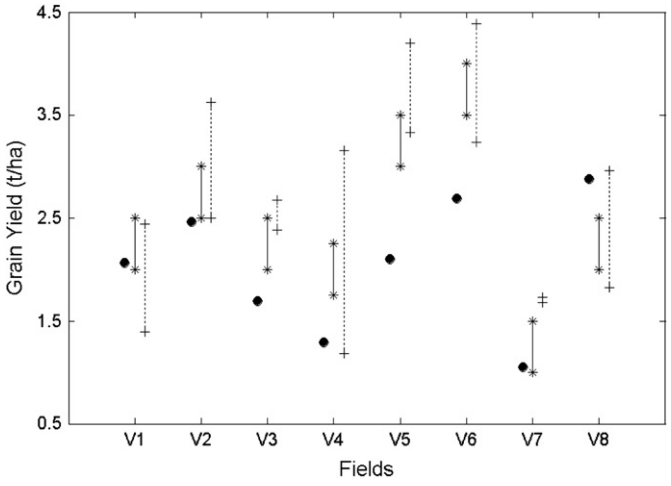

Fig. 10. Simulated values (black discs) of grain yield, together with ORMVAH estimates (vertical full lines) and field measurements (vertical dotted lines) on the validation fields. The length of full and dotted lines indicates the error associated to ORMVAH estimates and the standard deviation associated to measurements, respectively.

The problem may be due to the fact that the agricultural conditions on the calibration fields do not encompass those of the validation fields. In particular, the validation fields have been sown earlier and have received more irrigation water and fertiliser than the calibration fields. The model partly account for these variation because the GLAI was slightly larger on the validation than on the calibration fields: the simulations result in an average yield of 1.95 t ha^{-1} for fields V1 to V8 against 1.74 t ha^{-1} for fields C1 to C9. Nevertheless, re-calibration of the Py parameter would be necessary to obtain good estimate of grain yield for the 2003/2004 agricultural season.

5.4. Dry aerial mass

The dry aerial phytomass was measured on field V5 during the 2003/2004 agricultural season. The measurements of this variable are plotted against its simulation in Fig. 11. The performance of the SAFY model was surprisingly good since no specific calibration was performed for this variable. The agreement between observation and simulation is perfect at the beginning of the season (before day 150). The explanation is twofold: numerous GLAI observations are available to constrain the phytomass production and inaccuracy of measurements at high GLAI values does not strongly affect the phytomass production because of the saturation of PAR absorption (eq. 2). At the end of the season, the SAFY model clearly underestimates the dry aerial phytomass. This discrepancy appears to be due to the underestimation of grain yield. Globally, the SAFY model simulates the time course of dry aerial phytomass as accurately as others wheat models (e.g. Maas, 1993; O'Leary and Connor, 1996; Pala et al., 1996; Asseng et al., 1998; Jamieson et al., 1998; Olesen et al., 2002; Panda et al., 2003; Asseng et al., 2004; Wahbi and Sinclair, 2005). However, there is a need for evaluation on a wider range of crops and/or conditions to strengthen this conclusion.

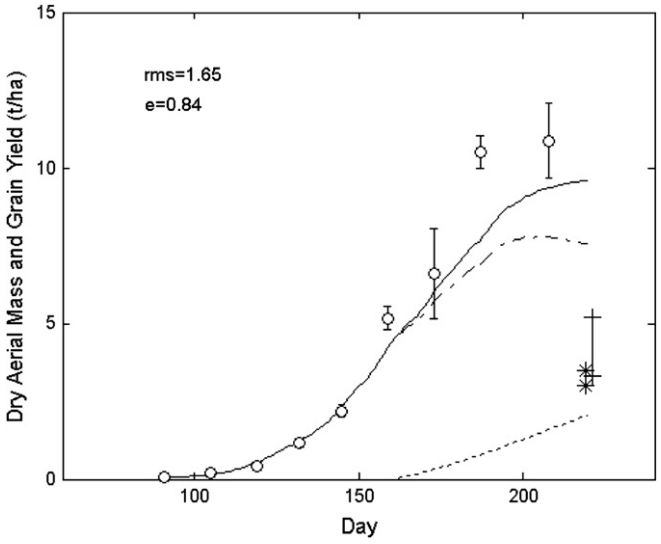

Fig. 11. Time courses of observed (stars) and simulated (full line) total dry above-ground phytomass on the V5 field. The root mean square error and the efficiency between measured and simulated values are displayed with label 'rms' and 'e', respectively. The dashed line corresponds to the dry mass of all aerial organs except grain. The dotted line displays the time course of simulated grain yield, associated with ORMVAH estimates and field measurement at the end of the season (vertical line with stars and plus symbols, respectively). The days are numbered from October 15, 2003.

6. Conclusion

The use of crop models on large areas for local (field scale) estimates of crop production is hampered by the lack of sufficient and accurate spatial information about model inputs. In particular it is impossible to exactly know the space and time variation of the input related to farmer practices (sowing, irrigation and fertilisation). As an alternative, a simple model (SAFY) was developed under the assumption that a key-parameter—the effective light-use efficiency—is sufficient to furnish an indicator of all agro-environmental stresses together. The model simulates the time courses of leaf area, dry above-ground phytomass and grain yield, with no explicit modelling of the effects of water or nutrient limitations on plant growth. The impact of possible water and nitrogen deficit is expected to be accounted for by the variation of the effective light-use efficiency, with the idea that this parameter can be derived from the time course of the green leaf area index (GLAI). This variable is critical in plant modelling, and a lot of techniques and methods are available for its observation by remote sensing from ground as well as from space. Since the model is based on a limited number of parameters and equations, its control with GLAI observations appears simple and robust. The approach offers the advantage to only describe well documented processes with standard data, i.e. data supplied by meteorological stations and time series of GLAI estimates which can be derived from satellite data. This makes it very attractive for operational application at a regional scale.

The approach was tested against field data collected on winter wheat during two successive agricultural seasons (2002/2004) in the plain that surrounds the city of Marrakech (Morocco). During this experiment 17 fields were monitored, with a large range of sowing dates as well as irrigation and fertilisation schedules. GLAI estimates were performed based on the NDVI collected at field using a handheld radiometer and the analysis of hemispherical photography. A method was developed to invert the two most sensitive parameters (date of emergence and effective light-use efficiency) from GLAI time courses at a field scale. The comparison of simulated/inverted and observed data has allowed us to reach the following conclusions:

- The retrieval of the dates of plant emergence appears satisfactory.
- The model provided with excellent simulations of the time courses of green leaf area index.
- Though no specific calibration was performed, the model accurately simulates the time course of the dry above-ground phytomass.
- Field-to-field variations of grain yield were also correctly predicted, but significant underestimation was observed

during evaluation. Underestimation was attributed to a shift in agricultural practices (irrigation and fertilisation) between the fields used for calibration (2002/2003) and those used for validation (2003/2004).

The last statement highlights the limit of the assumption prevailing in this study, which is the use of GLAI as an indicator of all agro-environmental stresses considered together. For grain yield prediction, strong attention should be paid at using the SAFY model close to its domain of calibration. The control of the model with satellite data (e.g. daily time series of images at high spatial resolution acquired by the new FORMOSAT-2 satellite) could result in accurate regional crop yield estimate provided that local measurements are available for calibration and that the agricultural practices do not much vary within the area of interest. Nevertheless, the SAFY model could be combined with remote sensing data to detect anomalies in crop phenology and to predict above-ground phytomass production at a regional scale. In particular, it could be used as a simple and accurate interpolator to monitor and/or predict the dynamics of the vegetation (green leaves). In this perspective it would be interesting to investigate the performance of the model in case of reduced GLAI data availability. The model can be also adapted to integrate additional processes associated to crop growth such as water transfer between soil, plant and atmosphere. SAFY was already coupled with the soil water balance and evapotranspiration models developed by the FAO to schedule irrigation (Duchemin et al., 2005). The assimilation of satellite data in the coupled model offers perspectives for the operational monitoring of crop actual evapotranspiration and water requirements at a regional scale.

Acknowledgements

This study was part of the SudMed project (www.irrimed.org/irri&;sudmed.htm) which involves IRD (*Institut de Recherche pour le Développement,* www.ird.fr), CESBIO (*Centre d'Etudes Spatiales de la Biosphère*, Toulouse, France, www.cesbio.ups-tlse.fr) and FSS (*Faculté des Sciences Semlalia*, Marrakech, Morocco, www.ucam.ac.ma). It was also funded by the European Commission through the 5th Framework INCO-MED program IRRIMED (www.irrimed.org). French CNRS-PNTS (*Programme National de Télédétection Spatiale*) and CNES-ISIS (*Incitation à l'utilisation Scientifique des Images SPOT*) programs are acknowledged for their support. The authors are indebted to SudMed regional partners who are in charge of water management in the Marrakech/Al Haouz plain, especially ORMVAH (*Office Régional de Mise en Valeur Agricole du Haouz*). The persons who participated in the collection of field data are gratefully acknowledged.

References

Allen, R.G., 2000. Using the FAO-56 dual crop coefficient method over an irrigated region as part of an evapotranspiration intercomparison study. Journal of Hydrology 229, 27–41.

Arora, V.K., Gajri, P.R., 1998. Evaluation of a crop growth-water balance model for analysing wheat responses to climate- and water-limited environments. Field Crops Research 59, 213–224.

Asseng, S., Keating, B.A., Fillery, I.R.P., Gregory, P.J., Bowden, J.W., Turner, N.C., Palta, J.A., Abrecht, D.G., 1998. Performance of the APSIM-wheat model in Western Australia. Field Crops Research 57, 163–179.

Asseng, S., Jamieson, P.D., Kimball, B., Pinter, P., Sayre, K., Bowden, J.W., Howden, S.M., 2004. Simulated wheat growth affected by rising temperature, increased water deficit and elevated atmospheric CO_2. Field Crops Research 85, 85–102.

Bastidas, L.A., Gupta, H.V., Sorroshian, S., Shuttleworth, W.J., Yang, Z.L., 1999. Sensitivity analysis of a land surface scheme using multicriteria method. Journal of Geophysical Research 104, 19,481–19,490.

Bastiaanssen, W.G.M., Molden, D.J., Makin, I.W., 2000. Remote sensing for irrigated agriculture: examples from research and possible applications. Agricultural Water Management 46, 137–155.

Beven, K.J., 2001. How far can we go in distributed hydrological modelling. Hydrology and Earth System Sciences 5, 1–12.

Beven, K.J., Binley, A.M., 1992. The future of distributed models: model calibration and uncertainty prediction. Hydrological Processes 6, 279–298.

Beven, K.J., Franks, S.W., 1999. Functional similarity in landscape scale SVAT modelling. Hydrology and Earth System Sciences 3, 85–94.

Boote, K.J., Jones, J.W., Pickering, N.B., 1996. Potential uses and limitations of crop models. Agronomy Journal 88, 704–716.

Brisson, N., Gary, C., Justes, E., Roche, R., Mary, B., Ripoche, D., Zimmer, D., Sierra, J., Bertuzzi, P., Burger, P., Bussière, F., Cabidoche, Y.M., Cellier, P., Debaeke, P., Gaudillère, J.P., Hénault, C., Maraux, F., Seguin, B., Sinoquet, H., 2003. An overview of the crop model STICS. European Journal of Agronomy 18, 309–322.

Chaponnière, A., Maisongrande, P., Duchemin, B., Hanich, L., Boulet, G., Escadafal, R., Elouaddat, S., 2005. A combined high and low spatial resolution approach for mapping snow covered area in the atlas mountain. International Journal of Remote Sensing 26, 2755–2777.

Chern, J.-S., Lee, L.-C., Wang, H.-C., Chu, F.-H., 2001. An Introduction to NSPO and ROCSATs Missions. 3rd IAA Symposium on Small Satellites for Earth Observation, Berlin, Germany, April 2-6, 2001.

Clevers, J.G.P.W., Vonder, O.W., Jonschaap, R.E., Desprats, J.F., King, C., Prévot, L., Bruguier, N., 2002. Using Spot data for calibrating a wheat growth model under Mediterranean conditions. Agronomie 22, 687–694.

Dedieu, G., Cabot, F., Chehbouni, A., Duchemin, B., Maisongrande, P., Boulet, G., Pellenq, J., 2003. RHEA: a micro-satellite mission for the study and modeling of land surfaces through assimilation techniques. EGS-AGU-EUG Joint Assembly, 6–11 April 2003, Nice (France).

Demarty, J., Ottle, C., Braud, I., Olioso, A., Frangi, J.P., Bastidas, L.A., Gupta, H.V., 2004. Using a multiobjective approach to retrieve information on surface properties used in a SVAT model. Journal of Hydrology 287, 214–236.

de Wit, A.J.W., Boogaard, H.L., van Diepen, C.A., 2004. Using NOAA-AVHRR estimates of land surface temperature for regional agrometeorogical modelling. International Journal of Applied Earth Observation and Geoinformation 5, 187–204.

de Wit, A.J.W., Boogaard, H.L., van Diepen, C.A., 2005. Spatial resolution of precipitation and radiation: The effect on regional crop yield forecasts. Agricultural and Forest Meteorology 135, 156–168.

Duan, Q., Sorooshian, S., Gupta, V., 1992. Effective and efficient global optimization for conceptual rainfall-runoff models. Water Resource Research 28, 1015–1031.

Duchemin, B., Boulet, G., Maisongrande, P., Benhadj, I., Hadria, R., Khabba, S., Chehbouni, A., Olioso, A., 14–17 Novembre 2005. Un modèle simplifié pour l'estimation du bilan hydrique et du rendement de cultures céréalières en milieu semi-aride. Deuxième Congrès Méditerranéen 'Ressources en Eau dans le Bassin Méditérranéen', Marrakech (Maroc).

Duchemin, B., Hadria, R., Erraki, S., Boulet, G., Maisongrande, P., Chehbouni, A., Escadafal, R., Ezzahar, J., Hoedjes, J.C.B., Kharrou, M.H., Khabba, S., Mougenot, B., Olioso, A., Rodriguez, J.-C., Simonneaux, V., 2006. Monitoring wheat phenology and irrigation in Central Morocco: on the use of relationships between evapotranspiration, crops

coefficients, leaf area index and remotely-sensed vegetation indices. Agricultural Water Management 79, 1–27.

Eitzinger, J., Trnka, M., Hösch, J., Žalud, Z., Dubrovský, M., 2004. Comparison of CERES, WOFOST and SWAP models in simulating soil water content during growing season under different soil conditions. Ecological Modelling 171, 223–246.

Faivre, R., Leenhardt, D., Voltz, M., Benoît, M., Papy, F., Dedieu, G., Wallach, D., 2004. Spatialising crop models. Agronomie 24, 205–217.

FAO, 2002. In: Deficit Irrigation Practices—Foreword. FAO Technical Papers—Water Reports No. 22. http://www.fao.org/documents/show_cdr.asp?url_file=/docrep/004/Y3655E/y3655e01.htm.

Franks, S.W., Beven, K.J., Quinn, P.F., Wright, I.R., 1997. On the sensitivity of soil-vegetation-atmosphere transfer (SVAT) schemes: equifinality and the problem of robust calibration. Agricultural and Forest Meteorology 86, 63–75.

Hadria, R., Khabba, S., Lahrouni, A., Duchemin, B., Chehbouni, A., Carriou, J., 2007. Calibration and validation of the STICS crop model for managing wheat irrigation in the semi-arid Marrakech/Al Haouz Plain. Arabian Journal for Science and Engineering 32, 87–101.

Jamieson, P.D., Porter, J.R., Goudriaan, J., Ritchie, J.T., van Keulen, H., Stol, W., 1998. A comparison of the models AFRCWHEAT2, CERES-Wheat, Sirius, SUCROS2 and SWHEAT with measurements from wheat grown under drought. Field Crops Research 55, 23–44.

Jonckheere, I., Fleck, S., Nackaerts, K., Muysa, B., Coppin, P., Weiss, M., Baret, F., 2004. Review of methods for in situ leaf area index determination. Part I. Theories, sensors and hemispherical photography. Agricultural and Forest Meteorology 121, 19–35.

Jørgensen, S.E., 1994. Models as instruments for combination of ecological theory and environmental practice. Ecological Modelling 75-76, 5–20.

Lobell, D.B., Asner, G.P., Ortiz-Monasterio, J.I., Benning, T.L., 2003. Remote sensing of regional crop production in the Yaqui Valley, Mexico: estimates and uncertainties. Agriculture. Ecosystems and Environment 94, 205–220.

Maas, S.J., 1993. Parameterized model of gramineous crop growth: I. Leaf area and dry mass simulation. Agronomy Journal 85, 348–353.

Meinke, H., Hammer, G.L., van Keulen, H., Rabbinge, R., 1998. Improving wheat simulation capabilities in Australia from a cropping systems perspective III. The integrated wheat model (I_WHEAT). European Journal of Agronomy 8, 101–116.

Mo, X., Liu, S., Lin, Z., Xu, Y., Xiang, Y., McVicar, T.R., 2005. Prediction of crop yield, water consumption and water use efficiency with a SVAT-crop growth model using remotely sensed data on the North China Plain. Ecological Modelling 183, 301–322.

Monteith, J.L., 1977. Climate and the efficiency of crop production in Britain. Philosphical Transactions of the Royal Society of London Ser. B 281, 277–294.

Moulin, S., Bondeau, A., Delécolle, R., 1998. Combining agricultural crop models and satellite observations from field to regional scales. International Journal of Remote Sensing 19, 1021–1036.

O'Connell, M.G., O'Leary, G.J., Whitfield, D.M., Connor, D.J., 2004. Interception of photosynthetically active radiation and radiation-use efficiency of wheat, field pea and mustard in a semi-arid environment. Field Crops Research 85, 111–124.

O'Leary, G.J., Connor, D.J., 1996. A Simulation Model of the Wheat Crop in Response to Water and Nitrogen Supply: II. Model Validation. Agricultural Systems 52, 31–55.

Olesen, J.E., Berntsen, J., Hansen, E.M., Petersen, B.M., Petersen, J., 2002. Crop nitrogen demand and canopy area expansion in winter wheat during vegetative growth. European Journal of Agronomy 16, 279–294.

Olioso, A., Inoue, Y., Ortega-Farias, S., Demarty, J., Wigneron, J.-P., Braud, I., Jacob, F., Lecharpentier, P., Ottlé, C., Calvet, J.-C., Brisson, N., 2005. Future directions for advanced evapotranspiration modeling: assimilation of remote sensing data into crop simulation models and SVAT models. Irrigation and Drainage Systems 19, 377–412.

Pala, M., Stockle, C.O., Harris, H.C., 1996. Simulation of durum wheat (*Triticum turgidum* ssp. *durum*) growth under different water and nitrogen regimes in a Mediterranean environment using CropSyst. Agricultural Systems 51, 147–163.

Panda, R.K., Behera, S.K., Kashyap, P.S., 2003. Effective management of irrigation water for wheat under stressed conditions. Agricultural Water Management 63, 37–56.

Pellenq, J., Boulet, G., 2004. A methodology to test the pertinence of remote-sensing data assimilation into vegetation models for water and energy exchange at the land surface. Agronomie 24, 197–204.

Porter, J.R., Gawith, M., 1999. Temperatures and the growth and development of wheat: a review. European Journal of Agronomy 10, 23–36.

Rodriguez, J.-C., Duchemin, B., Hadria, R., Watts, C., Garatuza, J., Chehbouni, A., Khabba, S., Boulet, G., Palacios, R., Lahrouni, A., 2004. Wheat yield estimation using remote sensing and the STICS model in the semiarid valley of Yaqui, Mexico. Agronomie 24, 295–304.

Scotford, I.M., Miller, P.C.H., 2005. Applications of spectral reflectance techniques in northern European cereal production: a review. Biosystems Engineering 90, 235–250, doi:10.1016/j.biosystemseng.2004.11.010.

Sinclair, T.R., Amir, J., 1992. A model to assess nitrogen limitations on the growth and yield of spring wheat. Field Crops Research 30, 63–78.

Szeicz, G., 1974. Solar radiation for plant growth. Journal of Applied Ecology 11, 617–636.

Tucker, C.J., 1996. History of the use of AVHRR data for land applications. In: D'Souza, G., et al. (Eds.), Advances in the Use of NOAA AVHRR Data for Land Applications. ECSC, EEC, EAEC, Brussels and Luxembourg.

Varlet-Grancher, C., Bonhomme, R., Chartier, M., Artis, P., 1982. Efficience de la conversion de l'énergie solaire par un couvert végétal. Acta Oecologia/Oecologia Plantarum 17, 3–26.

Verhoef, W., Bach, H., 2003. Remote sensing data assimilation using coupled radiative transfer models. Physics and Chemistry of the Earth 28, 3–13.

Vrugt, J.A., Diks, C.G.H., Bouten, W., Gupta, H.V., Verstraten, J.M., 2005. Towards a complete treatment of uncertainty in hydrologic modelling: combining the strengths of global optimisation and data assimilation. Water Resources Research 41, doi:10.1029/2004WR003059. W01017.

Vrugt, J.A., Gupta, H.V., Bouten, W., Sorooshian, S., 2002. A Shuffled Complex Evolution Metropolis algorithm for optimization and uncertainty assessment of hydrologic model parameters. Water Resources Research 39 (8), 1201, doi:10.1029/2002WR001642.

Wagener, T., Boyle, D.P., Lees, M.J., Wheater, H.S., Gupta, H.V., Sorroshian, S., 2001. A framework for development and application of hydrological models. Hydrology and Earth System Sciences 5, 13–26.

Wahbi, A., Sinclair, T.R., 2005. Simulation analysis of relative yield advantage of barley and wheat in an eastern Mediterranean climate. Field Crops Research 91, 287–296.

Wallach, D., Goffinet, B., Bergez, J.-E., Debaeke, P., Leenhardt, N.A.D., 2002. The effect of parameter uncertainty on a model with adjusted parameters. Agronomie 22, 159–170.

Weiss, M., Baret, F., Smith, G.J., Jonckheere, I., Coppin, P., 2004. Review of methods for in situ leaf area index (LAI) determination: Part II. Estimation of LAI, errors and sampling. Agricultural and Forest Meteorology 121, 37–53.

Welles, J.M., Norman, J.M., 1991. Instrument for indirect measurement of canopy architecture. Agronomy journal 83, 818–825.

Xue, Q., Weiss, A., Stephen Baenziger, P., 2004. Predicting leaf appearance in field-grown winter wheat: evaluating linear and non-linear models. Ecological Modelling 175, 261–270.